Generalized Langevin-Debye model of the field dependence of tilt, birefringence, and polarization current near the de Vries smectic-A^* to smectic-C^* liquid crystal phase transition

Yongqiang Shen,[1] Lixing Wang,[2] Renfan Shao,[1] Tao Gong,[2] Chenhui Zhu,[1] Hong Yang,[2,*]
Joseph E. Maclennan,[1] David M. Walba,[2] and Noel A. Clark[1,†]

[1]*Department of Physics, and the Liquid Crystal Materials Research Center, University of Colorado, Boulder, Colorado 80309, USA*
[2]*Department of Chemistry and Biochemistry, and the Liquid Crystal Materials Research Center, University of Colorado, Boulder, Colorado 80309, USA*

(Received 24 July 2013; published 10 December 2013)

In chiral smectic-A (Sm-A) liquid crystals, an applied electric field induces a tilt of the optic axis from the layer normal. When these materials are of the de Vries type, the electroclinic tilt susceptibility is unusually large, with the field-induced director reorientation accompanied by a substantial increase in optical birefringence with essentially no change in the smectic layer spacing. In order to account for the observed electro-optic behavior, we assume that the molecular orientation distribution in the Sm-A has two degrees of freedom: azimuthal orientation and tilt of the molecular long axis from the layer normal, with the tilt confined to a narrow range of angles. We present a generalized Langevin-Debye model of the response of this orientational distribution to applied field that gives a field-induced optic axis tilt, birefringence, and polarization dependence that agrees well with experimental measurements and reproduces the double-peaked polarization current response characteristic of a first-order Sm-A^*–Sm-C^* transition. Additionally, we find that the measured field-induced polarization and the Langevin-Debye model predictions can be quantitatively described as pre-transitional behavior near the tricritical point of a recently published generalized 3D XY model of interacting hard rods confined to reorient on a cone in the presence of an applied field.

DOI: 10.1103/PhysRevE.88.062504 PACS number(s): 61.30.Cz, 61.30.Gd, 77.80.Fm, 78.20.Jq

Fluid smectic liquid crystal phases of chiral molecules exhibit a chiral coupling of molecular tilt to bulk polarization density [1]. In tilted chiral smectics, such as the Sm-C^* phase of rod-shaped molecules, this leads to an equilibrium macroscopic polarization, **P**, in each smectic layer which is oriented parallel to the layer plane and normal to the tilted molecular director, **n**, corresponding to the mean molecular long axis. Polar ordering is also observed in the tilted (Sm-C-like) and orthogonal (Sm-A-like) phases of both chiral and nonchiral bent-core liquid crystals [2–4]. In general, polar smectics respond to applied field, **E**, by reorientation of the coupled director-polarization fields, described by their variable azimuthal orientation, $\phi(\mathbf{r}, t)$, about the layer normal, **z**.

The layer polarization in bulk smectics can be organized in a variety of ways, with observations of ferroelectric, antiferroelectric, and ferrielectric phases reported [5]. A method widely used for probing the nature of the polar ordering is applying a time-varying electric field to the sample and measuring the resulting polarization current, $i = dP/dt$. For a linearly varying applied field, such as a triangle wave, the polarization current response of a polar smectic is generally highly nonlinear. The antiferroelectric phase is characterized by current peaks at symmetric threshold applied voltages above and below zero, marking the transitions between the antiferroelectric ground state and the field-induced ferroelectric states [6]. Polar phase materials, on the other hand, often referred to as ferroelectrics, typically exhibit only a single peak accompanying the reorientation of ϕ, either at finite voltage or centered at $V = 0$ [7,8].

Polarization current may also be used to investigate paraelectric smectics such as the Sm-A^* phase of chiral, rod-shaped molecules, in which **n** is along **z** in the absence of an external field but tilts through an angle ψ when an electric field is applied, a response known as the electroclinic effect [9]. In typical (non-de Vries) Sm-A^* materials, the tilt susceptibility is largest at $E = 0$ and the induced current varies with E roughly as a Langevin function, i.e., $i(t) = dP/dt \sim d[P_0 \tanh(E/kT)]/dt$. This current has a maximum at $E = 0$ and is nearly independent of E for small-susceptibility materials (or small applied fields). In materials with large electroclinic susceptibility, saturation of the induced tilt occurs at readily achieved fields and with a triangular voltage applied, the current response typically has a single peak centered about the zero crossing of the applied voltage.

In this paper we describe in detail the electro-optic and polarization current response of chiral de Vries smectics A, orthogonal phases in which the molecular cores are substantially tilted but have no azimuthal coherence in the tilt beyond local correlations [10,11]. The molecular dipole orientations in these materials are isotropically distributed in the layer plane and there is no net polarization in the absence of field. Applied electric fields, however, couple to the polarization, competing with the orientational entropy and inducing azimuthal anisotropy by confining the polarization distribution to an ever narrower range of ϕ values with increasing E. This induction of in-plane orientational order results in an increase in the birefringence and a large electroclinic tilt, electro-optic behavior that is well described by a generalized Langevin-Debye model with a field-dependent tilt distribution, as we will demonstrate below.

*Current address: School of Chemistry and Chemical Engineering, Southeast University, Nanjing, 211189, China.
†noel.clark@colorado.edu

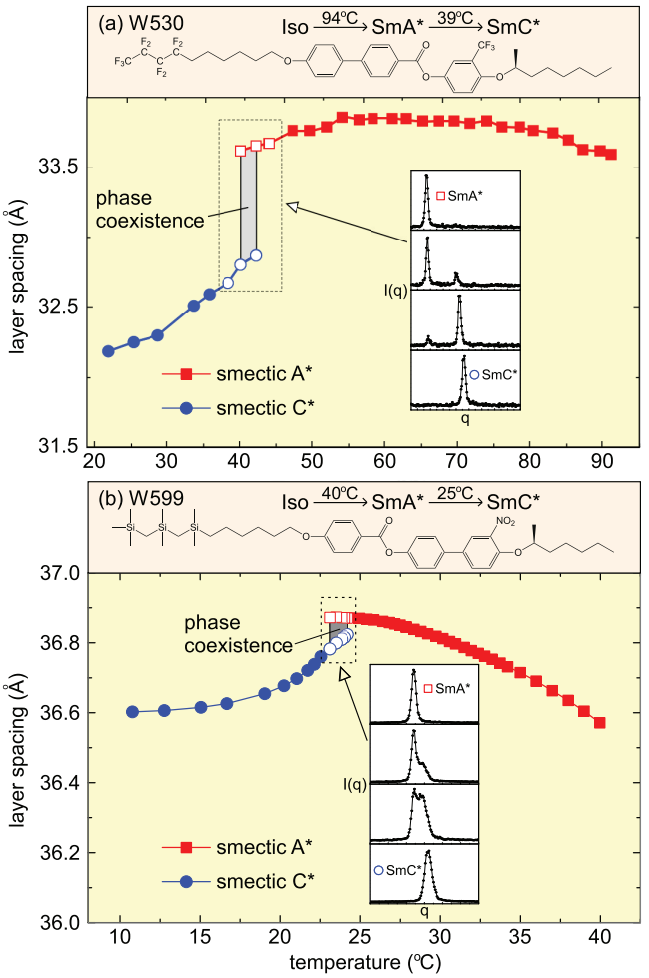

FIG. 1. (Color online) Molecular structure, phase diagrams, and temperature dependence of the layer spacing of (a) W530 and (b) W599. X-ray diffraction experiments on powder samples were carried out on beamline X10A of the National Synchrotron Light Source at Brookhaven National Laboratory (wavevector resolution $\delta q \sim 0.0004$ Å^{-1}). The insets show selected x-ray scattering profiles across the Sm-A^*–Sm-C^* phase transition.

The structures of the two chiral de Vries materials studied in this paper, W530 and W599, are shown in Fig. 1. The molecules have similar cores with a chiral alkoxy group on one end; W530 has a terminal perfluorinated decyloxy tail on the other end, while W599 has a carbosilane tail. These tails suppress out-of-layer fluctuations, which results in well-defined smectic layering, a characteristic known to promote de Vries behavior [11]. We have measured the layer spacing by high-resolution synchrotron x-ray diffraction on powder samples of W530 and W599. These materials show small layer contractions of only 4.3% and 0.73%, respectively, 10°C below the Sm-A^* to Sm-C^* phase transition (Fig. 1). In the de Vries picture, this minimal layer shrinkage is evidence that the molecules are tilted on a cone of angle θ_A in the Sm-A^* phase, with a random azimuthal distribution of ϕ that becomes biased along one direction at the Sm-A^*–Sm-C^* transition. The "de Vries character" of a liquid crystal material can be expressed by the reduction factor $R = \delta(T)/\theta_{\rm opt}(T) = \cos^{-1}[d_C(T)/d_{AC}]/\theta_{\rm opt}(T)$, where $\delta(T)$ is the

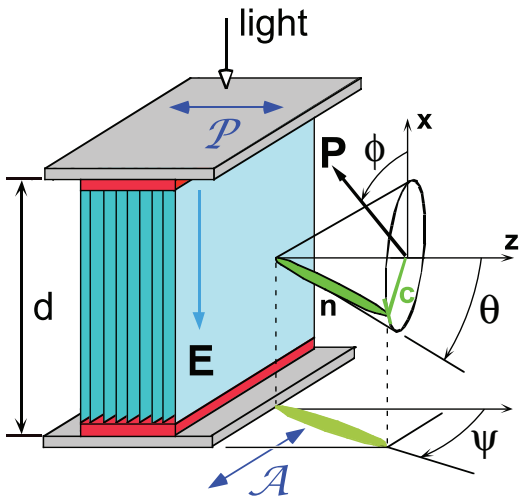

FIG. 2. (Color online) Electro-optic geometry, showing a representative molecule in the de Vries Sm-A^* phase in a bookshelf cell with ITO-coated glass substrates (gray) and nylon alignment layers (red). The smectic layers are oriented perpendicularly to the substrates and the molecule is tilted from the layer normal **z** by an angle θ. The polarization **P** is locally normal to the tilt plane (defined by the molecular long axis orientation **n** and **z**) and makes an angle ϕ relative to the cell normal **x**. The projection of the effective optic axis onto the plane of the cell subtends an angle ψ with the layer normal. The electro-optic response is measured in transmission, using normally incident light and with the cell between crossed polarizer and analyzer as shown.

tilt angle required to give the layer contraction relative to the layer spacing d_{AC} at the Sm-A^*–Sm-C^* transition and $\theta_{\rm opt}(T)$ is the optical tilt angle measured by polarized optical microscopy [12]. According to this expression, a material would approach the defect-free, bookshelf geometry in the Sm-C^* phase as $R \to 0$. The R values for W530 and W599 at $T = T_{AC}$-10°C are 0.39 and 0.18, respectively, which are typical for de Vries materials [13]. Selected x-ray scattering profiles of W530 and W599 near the Sm-A^*–Sm-C^* phase transition are shown in the insets of Figs. 1(a) and 1(b). Two separate peaks from lamellar reflections can be distinguished in a narrow temperature range around the phase transition, confirming the coexistence of the Sm-A^* and Sm-C^* phases and providing strong evidence that the Sm-A^* to Sm-C^* transition in both W530 and W599 is first order, a characteristic property of de Vries materials.

We studied the electro-optics of both materials in ITO-glass cells with the liquid crystal aligned in the bookshelf geometry, as illustrated in Fig. 2. In order to obtain uniform alignment, both substrates were coated with nylon but only one was rubbed. An electric field applied to the cell gives rise to an electroclinic response, with the optic axis tilting in response to the field and breaking the axial symmetry of the Sm-A^* phase. Measurements were carried out with the cell between crossed polarizer and analyzer, with the polarizer along the smectic layer normal.

The optical transmission and polarization reversal current response of W530 to a triangular applied voltage (of amplitude 110 V across a 2.3-μm-thick cell) are plotted in Fig. 3. At high temperatures in the Sm-A^* phase [Fig. 3(a)], where the

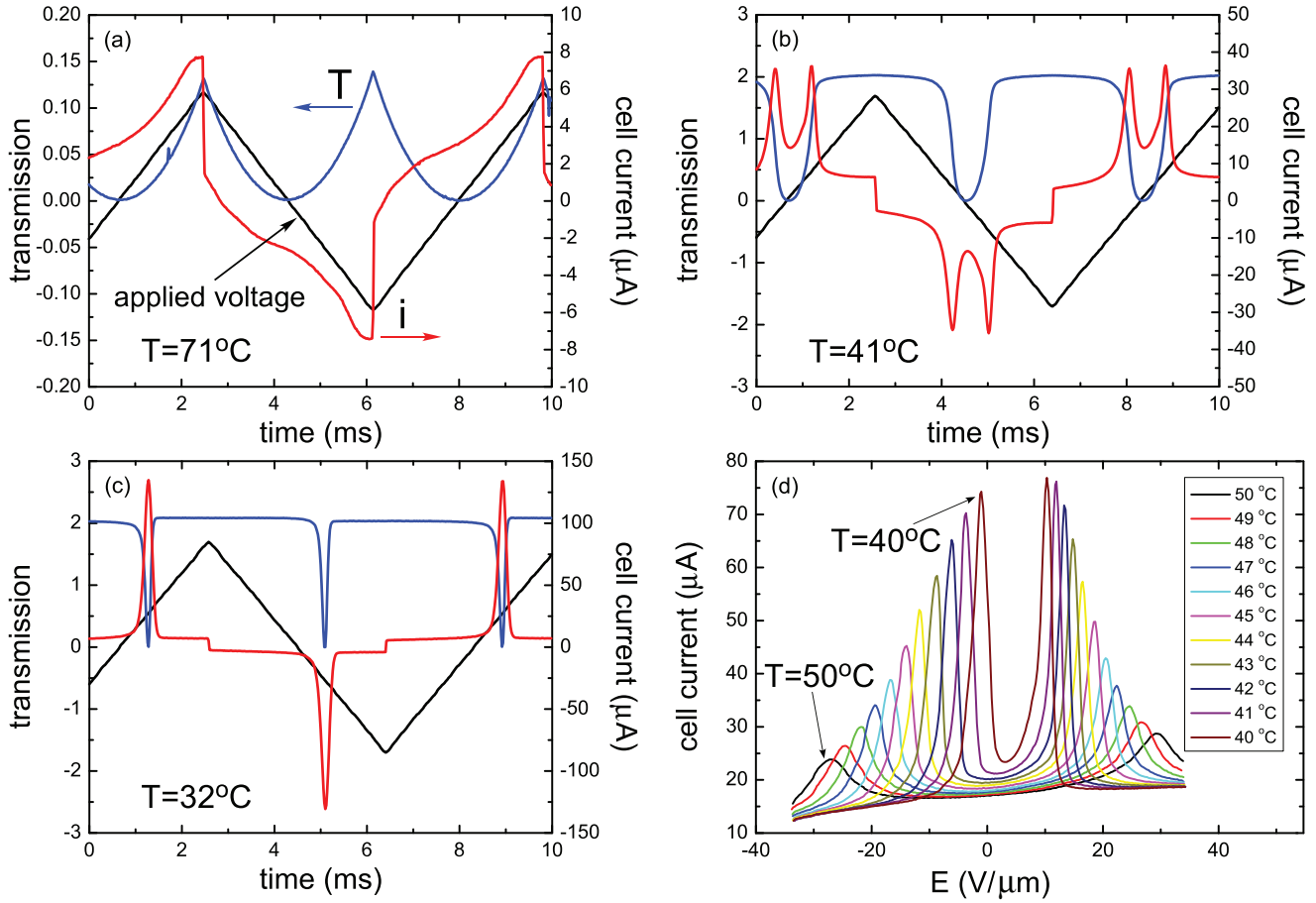

FIG. 3. (Color online) Electro-optic and current response of W530 in a 2.3-μm-thick cell with ITO electrodes. The applied voltage is a 100-Hz triangle wave with amplitude 110 V. (a) Sm-A^* phase response at high temperature. The applied field is too weak to produce discernible polarization current peaks. (b) Sm-A^* phase response at low temperature. Double peaks due to reorientation of the polarization are seen in the current response here. (c) Sm-C^* phase response, showing V-shaped optical transmission and single current peaks. The driving voltage in these plots is shown in black, the polarization current in red, and the optical transmission in blue. (d) Current response vs applied field at different temperatures in the Sm-A^* phase. The current shows two peaks symmetric about the $E = 0$ crossing that get closer together and increase in amplitude on cooling.

electroclinic susceptibility $\chi = \psi/E$ is small, the applied field is sufficient only to perturb the azimuthal orientational distribution of the molecules slightly. The change in optical transmission is small and there is no detectable polarization current peak at these temperatures. On cooling, however, the electroclinic susceptibility increases and the applied field can then switch the molecules essentially completely to a single azimuthal orientation and saturate the electro-optic response [Fig. 3(b)]. The polarization reversal current in this temperature range is symmetric and double peaked, a response that differs substantially from the constant or single-peak current response at the zero voltage crossing expected in a conventional Sm-A^* phase material [5]. We first reported double-peak polarization current in the de Vries Sm-A^* phase of W530 [14]. Prasad *et al.* [15] and Ghosh *et al.* [16] subsequently described similar behavior in other de Vries materials and proposed that the double peaks pointed to an underlying antiferroelectric structure. Double peaks in the polarization current response to an applied triangle wave voltage are certainly observed in the antiferroelectric Sm-C^*_A phase [17], as well as in the Sm-C^* phase when the helix pitch is short [18–20]. The double peaks in the present case do not imply antiferroelectricity but are the signature of a first-order Sm-A^*–Sm-C^* phase transition [21,22].

Finally, in the Sm-C^* phase [Fig. 3(c)], the field-induced azimuthal rotation of the director on the tilt cone (the Goldstone mode) yields a minimum in the transmission when the projection of the director onto the plane of the cell is along **z**, as is the case in the field-off state in both materials studied here. When the driving voltage is small, the optical transmission is linear in applied field, giving a characteristic "V-shaped" response [23], and there is a single current peak near the zero crossing of the applied voltage.

The polarization current response in the de Vries Sm-A^* phase depends strongly on temperature. As we have already seen, with a triangular applied voltage of amplitude 110 V there is no detectable polarization current peak at high temperatures in the Sm-A^* phase of W530. On cooling, the tilt starts to show saturation behavior at high field at around 54°C and a clear double-peak current profile becomes apparent. At first the current peaks are small and widely separated, but on further cooling towards the Sm-C^* phase, they increase in

amplitude and move closer together, as illustrated in Fig. 3(d), corresponding to the point of inflection in the $P(E)$ curve moving to lower applied voltage. In principle, a double-peak current response would be obtained over the entire Sm-A^* range of W530 if a high-enough voltage were applied to the cell. In practice, though, the cell is easily damaged when the applied field is too large. The Sm-A^* temperature range of W599 is narrower than that of W530, and in this material we do observe a double-peaked current response throughout the Sm-A^* phase range with the given field.

We performed detailed measurements of the induced apparent optical tilt and birefringence of W530 and W599 at different temperatures, plotted as symbols in Figs. 4(a) and 4(b). In both materials, the magnitude of the induced tilt increases with electric field strength and reaches saturation more quickly the lower the temperature. W530 has a fairly broad Sm-A^* temperature range (∼55°C wide). It is evident that the electroclinic response of W530 strengthens significantly on cooling, evolving from a linear response at temperatures far above the Sm-A^*–Sm-C^* phase transition to a distinctly sigmoidal response at the lower end of the Sm-A^* phase, with a field-dependent tilt susceptibility that is larger for intermediate values of ψ ($5^\circ < \psi < 25^\circ$) than for lower or higher induced tilts. The temperature range of the Sm-A^* phase of W599, on the other hand, is relatively narrow (∼15°C) and the electroclinic tilt curves show sigmoidal character throughout the Sm-A^* range. Field-induced reorientation of the optic axis is accompanied in the de Vries Sm-A^* phase by an increase in the birefringence. In the absence of applied field, the molecules have a random azimuthal distribution, the net polarization is zero, and the effective birefringence is reduced by orientational averaging. When an electric field is applied to the liquid crystal, the molecular dipoles couple to the field and their azimuthal distribution becomes anisotropic, the molecules becoming more aligned along a preferred direction normal to the field. This leads to tilting of the effective optic axis projected onto the plane of the cell and to an increase in the cell birefringence. As the temperature decreases, on approaching the Sm-C^* phase, it becomes easier to align the molecules using the applied field and the birefringence saturates more readily.

The principal theoretical approach that has been used to explain the unusual electro-optic characteristics of de Vries materials is derived from the Langevin-Debye model [24–26] proposed by Fukuda as a way of explaining the paradoxical "thresholdless antiferroelectricity" apparently observed in some chiral tilted smectic phases [27]. Although these phases were later shown to be Sm-C^* [28], Clark *et al.* demonstrated that the Langevin-Debye approach could be used with some success to describe key elements of the observed electro-optic behavior of de Vries materials [25]. This original model assumes that in the de Vries Sm-A^* phase in the absence of applied electric field, the molecules are azimuthally randomly distributed on a fixed tilt cone of angle θ_A, and in an applied field $\mathbf{E}$, the local dipole moment $\mathbf{p}$ couples ϕ to $\mathbf{E}$ with an energy $U_p = -pE\cos\phi$. With this minimal description of the free energy, a Langevin-Debye model qualitatively reproduces many of the features of the electro-optic response but does not give the sigmoidal response curves associated with the experimentally observed first-order nature of the phase transition. While reproducing the observed general trend of increasing Δn and ψ as the applied field is increased, this simple model tends to underestimate Δn at low fields (and underestimate ψ at high fields) [24,25,29]. Here we describe a modified Langevin-Debye model with an orientation distribution in which not only is there an azimuthal degree of freedom but the tilt θ is allowed to vary with applied field over a prescribed range, driven by a free energy term quadratic in the electric field, a feature which dramatically improves the agreement between theory and experiment. The free energy in this generalized model may be expressed as

$$\begin{aligned} U &= -\mathbf{p}\left(1+\alpha\frac{\mathbf{p}}{|\mathbf{p}|}\cdot\mathbf{E}\right)\cdot\mathbf{E} \\ &= -p_0E\sin\theta\cos\phi(1+\alpha E\cos\phi), \end{aligned}$$

where $p = p_0\sin\theta$ is the magnitude of the dipole moment of a tilt correlation domain. The term linear in electric field in this expression, $-p_0E\sin\theta\cos\phi$, describes the usual dipole interaction energy and appeared in the original model. The new quadratic term, $-\alpha p_0E^2\sin\theta\cos^2\phi$, which scales with the phenomenological parameter α, gives a tilt susceptibility that increases with field and leads to a sigmoidal response to applied field. The tilt angle $\psi(E)$ and birefringence $\Delta n(E)$ are given by

$$\tan 2\psi = \frac{\langle\sin 2\theta\cos\phi\rangle}{\langle\cos^2\theta-\sin^2\theta\cos^2\phi\rangle}, \tag{1}$$

$$\frac{\Delta n}{\Delta n_{\max}} = \frac{\langle\cos^2\theta-\sin^2\theta\cos^2\phi\rangle}{\cos 2\psi}. \tag{2}$$

The averages $\langle X\rangle$ are evaluated over the molecular orientation distribution according to $\langle X\rangle = \int_{\theta_{\min}}^{\theta_{\max}}\int_0^{2\pi} X(\theta,\phi)f(\theta,\phi)\sin\theta d\theta d\phi$, where $f(\theta,\phi) = \exp[-U/k_BT]/\int_{\theta_{\min}}^{\theta_{\max}}\int_0^{2\pi}\exp[-U/k_BT]\sin\theta d\theta d\phi$ is the mean-field orientation distribution function. Details of the derivation of Eqs. (1) and (2) are given in the appendix. The tilt angle $\theta(E)$ is allowed to vary in this model between a value inferred from the measured zero-field birefringence and the maximum tilt angle measured in a large applied field, where the birefringence is assumed to be saturated. For W530, we found these limits to be $\theta_{\min} = 17.8^\circ$ and $\theta_{\max} = 33.4^\circ$ and for W599 $\theta_{\min} = 25.6^\circ$ and $\theta_{\max} = 33.7^\circ$. By way of illustration, we show the model distribution function for W599 at T = 29°C for several different applied electric fields in Fig. 5. In the absence of field, ϕ is uniformly distributed between -180° and 180°, with θ uniformly distributed between $\theta_{\min} = 25.6^\circ$ and $\theta_{\max} = 33.7^\circ$. As the applied field becomes stronger, $f(\theta, \phi)$ becomes increasingly peaked, with the molecules eventually being confined to a single azimuthal orientation and having maximal tilt.

Fits to the experimental tilt angle and birefringence using Eqs. (1) and (2) are plotted in Figs. 4(a) and 4(b). The variation of the fitting parameters α and p with temperature is indicated in Figs. 4(c) and 4(d). As we will see below, the similarity of the behavior predicted by this model is similar to the field response of a model first-order 3D XY system [30]. In both cases, the nonlinear increase of susceptibility with increasing field, ultimately limited by the saturation of the orientation at $\phi = 0^\circ$, gives a sigmoidal response to applied field characteristic of de Vries materials. The magnitude of the local dipole moment

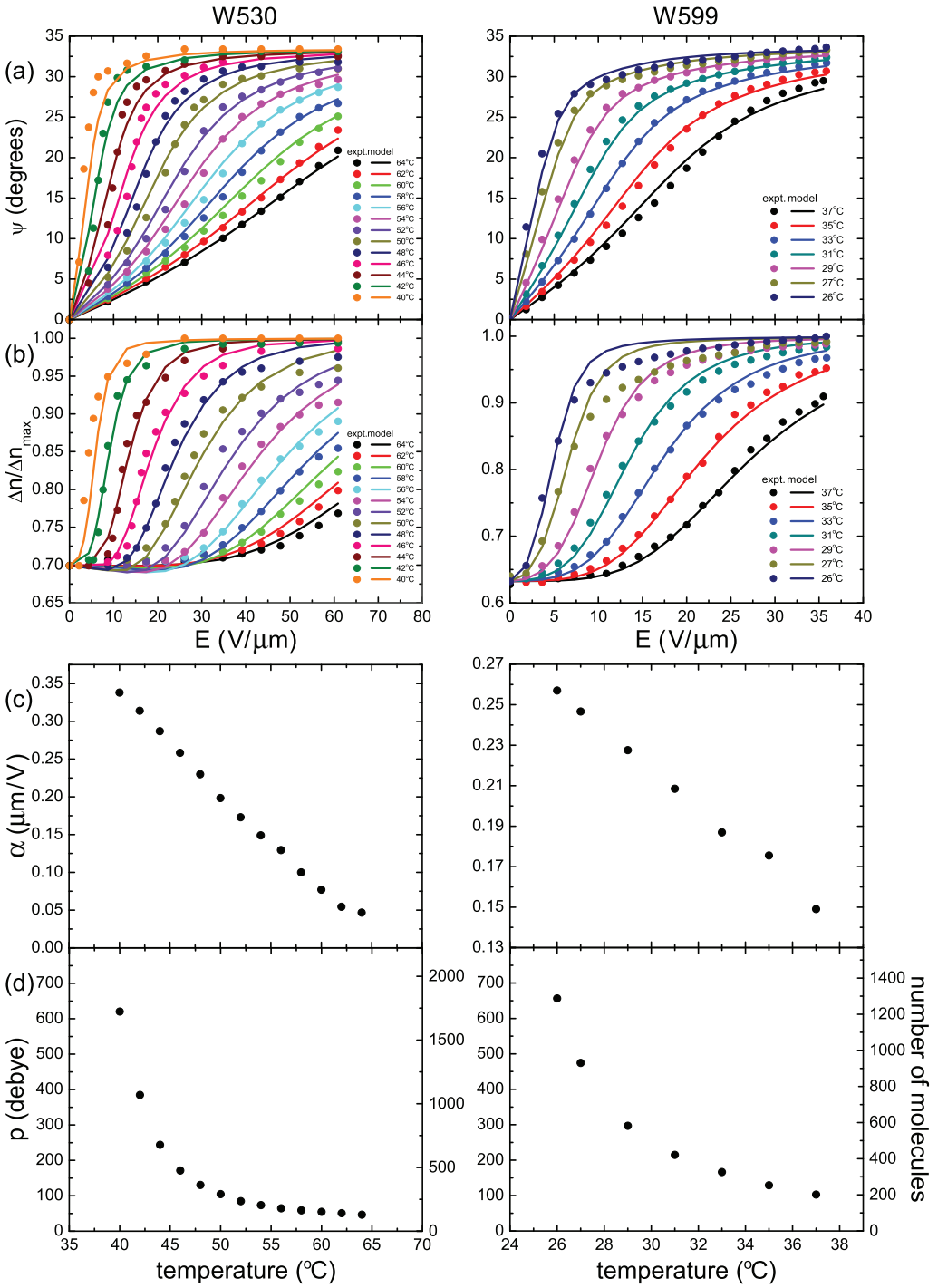

FIG. 4. (Color online) Electro-optic response of W530 (left) and W599 (right) in the Sm-A^* phase. (a) Measured field-induced optical tilt (symbols) fitted with generalized Langevin-Debye model (lines). (b) Measured field-induced birefringence and model fits. At high temperatures, the electro-optic response shows positive curvature over the entire range of available applied electric field but the response becomes sigmoidal on cooling (for $T \lesssim 58^\circ$C in W530 and for $T \lesssim 37^\circ$C in W599). Temperature dependence of the magnitudes of (c) the phenomenological parameter α and (d) the local dipole moment p given by the fits. In (d) we also indicate the number of molecules in each correlation domain (right axis).

p in the Langevin-Debye model diverges on approaching the Sm-A^*–Sm-C^* transition, corresponding to growth of the tilt correlation domains. The effective molecular dipole moments of W530 and W599 estimated from the saturated polarization densities and assuming a liquid crystal mass density of 1.2 g/cm^3 are 0.36 D and 0.51 D, respectively, from which we can estimate that the correlated tilt domains in W530 (W599) grow on cooling through the Sm-A^* temperature range from just a few molecules at high temperature to include around 1720 (1280) molecules near the Sm-C^* transition. This

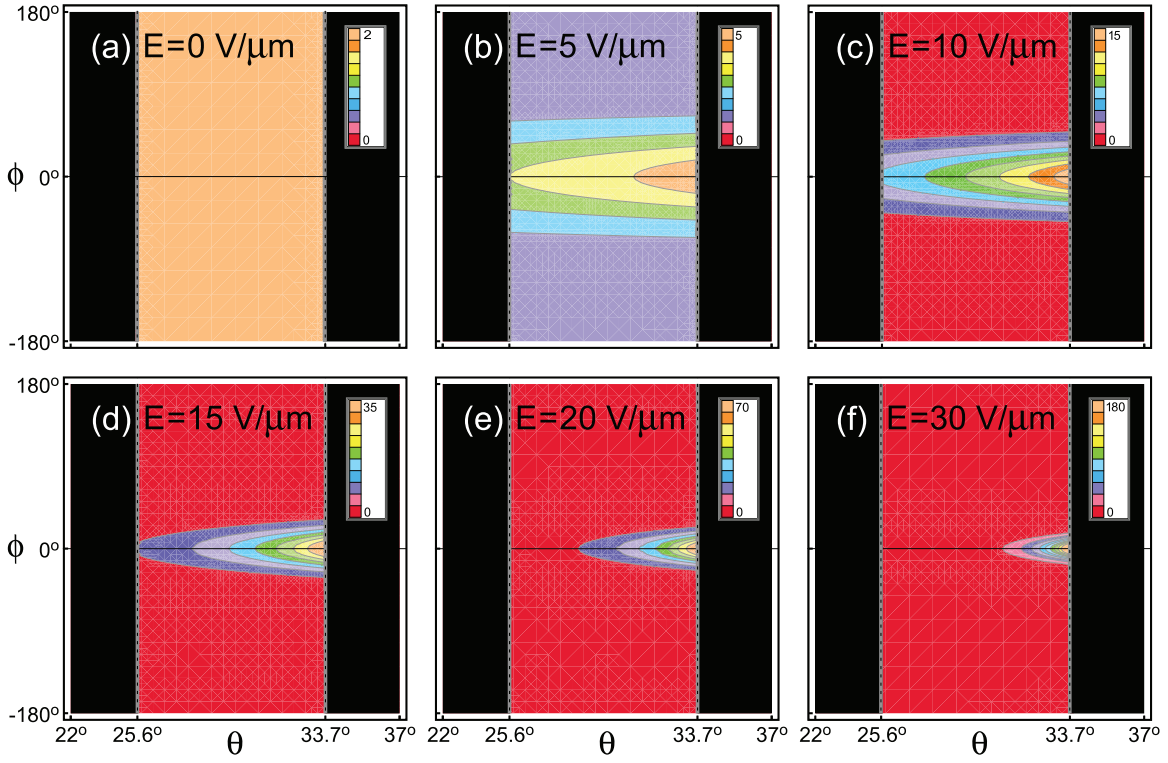

FIG. 5. (Color online) Orientation distribution function $f(\theta, \phi)$ used in the generalized Langevin-Debye model for W599 at $T = 29°$C and selected applied electric field strengths: (a) 0 V/μm, (b) 5 V/μm, (c) 10 V/μm, (d) 15 V/μm, (e) 20 V/μm, and (f) 30 V/μm.

result is similar to estimates made by Selinger *et al.*, who found, using a different model, that the correlation domains near the Sm-A^*–Sm-C^* transition in two de Vries materials closely related to those studied here comprised on the order of a few thousand molecules [24].

The experimental values of $\Delta n/\Delta n_{\max}$ vs ψ^2 measured at different temperatures in the de Vries Sm-A^* phase fall essentially on a single trajectory, as can be seen in Fig. 6. The original Langevin-Debye model previously developed by Clark *et al.* [25], which assumed a constant cone angle θ_A, reproduces this experimental behavior only qualitatively: if the cone angle is set to the value required to match the birefringence at zero field (26.6° in W530, 29.6° in W599), this model [green dashed lines in Figs. 6(a) and 6(b)] deviates from experiment at high fields; if θ_A is set instead to be the maximum measured tilt angle (33.4° in W530, 33.7° in W599), the model [red dashed lines in Figs. 6(a) and 6(b)] deviates at small fields. This observation motivated the development of a model in which the tilt distribution depends on the applied field, described in detail here. This generalized model yields fits, shown as solid lines in Fig. 6, that have little dependence on temperature and agree quite well with the experimental measurements of $\Delta n/\Delta n_{\max}$ vs ψ^2. The model curves have the same starting and ending points at all temperatures, in

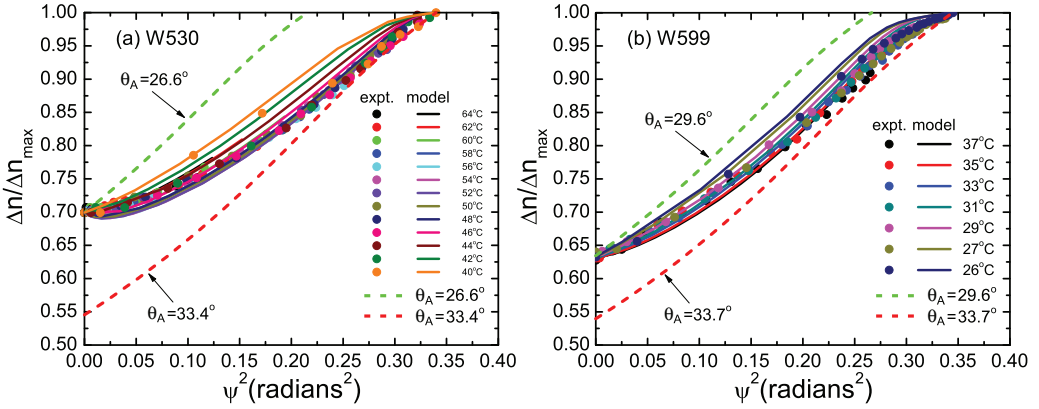

FIG. 6. (Color online) Birefringence variation with induced optical tilt in the de Vries Sm-A^* phase of (a) W530 and (b) W599. The experimental trajectories (symbols) are essentially independent of temperature. The original Langevin-Debye model with fixed tilt cone θ_A (green and red dashed lines) does not reproduce the observed field dependence, while the generalized model (solid lines) fits well.

agreement with experiment, and reflect the observed increase of optical tilt with applied field.

Since the macroscopic polarization $P = \int i dt/A = \int i dE/(A dE/dt)$, P can be determined directly by integrating the experimental polarization reversal current $i(E)$, shown as symbols in Fig. 7. The polarization is given theoretically in the generalized Langevin-Debye model by

$$P = \frac{P_{\max}\langle \sin\theta \cos\phi \rangle}{\sin\theta_{\max}}, \tag{3}$$

where $P_{\max}$ and $\theta_{\max}$ are the maximum polarization and tilt angle just above the Sm-A^*–Sm-C^* transition. For W530, we found $P_{\max} = 110$ nC/cm^2, and for W599, $P_{\max} = 165$ nC/cm^2. When we calculate the polarization $P(E)$ from Eq. (3) using the fitting parameters α and p obtained previously, the theoretical values match experiment well for both W530 and W599 over the entire temperature range in which double peaks appear in the current response, as shown in Figs. 7(a) and 7(b). This result confirms that the generalized Langevin-Debye model provides a self-consistent description of the electro-optic response of de Vries Sm-A^* materials.

All of the experimental and calculated P vs E curves in Figs. 7(a) and 7(b) have sigmoidal character. Since the polarization reversal current $i \propto dP/dE$, a current peak is observed wherever $d^2P/dE^2 = 0$. Since $P(E)$ is sigmoidal and has odd symmetry, a current peak appears both before and after the zero crossing. Antiferroelectric ordering of **P** is clearly not necessary to produce this effect. As is evident in Figs. 7(a) and 7(b), when $E = 0$, dP/dE is nonzero and the polarization current is finite. When E is very large, the optical tilt saturates, the polarization stops changing with increasing field strength, and the polarization current drops to zero. The electroclinic susceptibility increases substantially on cooling and the optical tilt saturates more readily with applied field, causing the current peaks to move closer to the zero voltage crossing and increase in amplitude as the temperature is lowered, as illustrated in Fig. 3(d).

Recently, Kost-Smith *et al.* [30] developed a generalized 3D XY model of de Vries materials and demonstrated that the steric interactions inherent in the hollow-cone de Vries model can produce a first-order Sm-A^*–Sm-C^* phase transition, which leads to a sigmoidal field response as seen experimentally. Fits to the polarization field response of W530 with this model, shown in Fig. 7(c), are similar to ours. In the 3D XY model, on cooling to the phase transition, the polarization first varies continuously with field and shows sigmoidal behavior, but the response becomes discontinuous on approaching the transition, with the first-order threshold field becoming lower on cooling. In our experiments on W530 and W599, the field-induced tilt and birefringence curves are continuous at all temperatures as imperfections in the alignment prevent observation of any field-induced phase change domains at low temperature (although this is observed in other materials [25]). The generalized Langevin-Debye model curves show similar behavior, with a linear response at high temperature that becomes sigmoidal on cooling. In both the Langevin-Debye and 3D XY models, the polarization saturates at high field because once the tilt saturates, no further increase of the polarization is possible. Remarkably, the evolution of the electro-optic response and the temperature range over which the tilt susceptibility grows, both fixed in the 3D XY model once its interaction parameter is set to give the Sm-A–Sm-C transition temperature, accounts accurately for the field and temperature dependence.

In summary, we have investigated two de Vries liquid crystal materials with first-order Sm-A^*–Sm-C^* phase

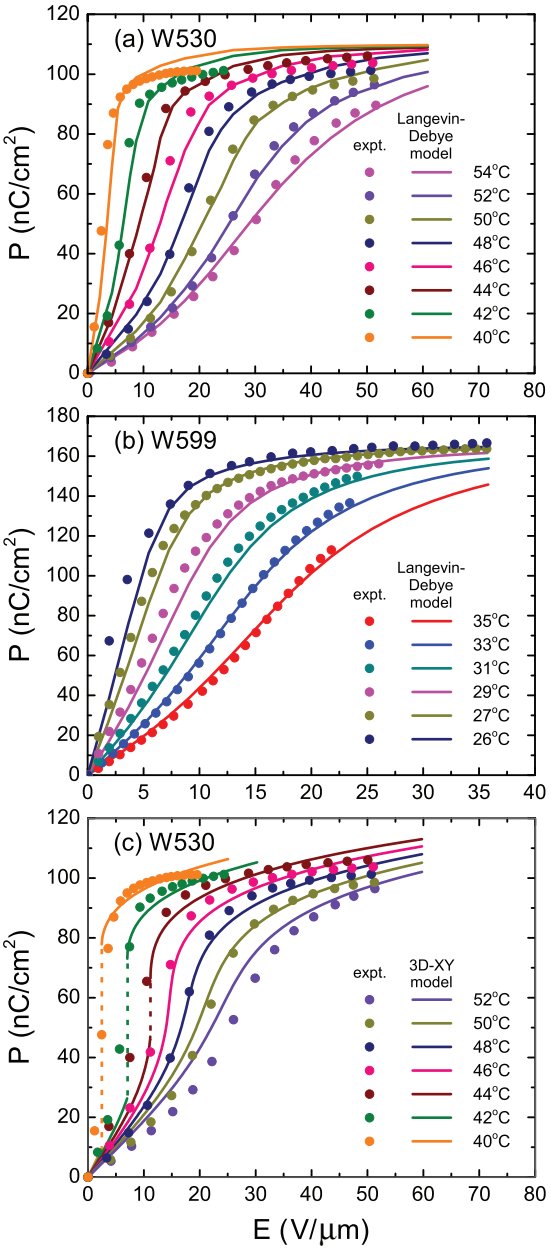

FIG. 7. (Color online) Measured and calculated induced polarization of (a) W530 and (b) W599 vs applied electric field at different temperatures in the Sm-A^* phase. The experimental values are obtained by integrating the polarization reversal current while the theoretical curves are computed using the generalized Langevin-Debye model. The polarization values inferred from fitting the electro-optic data using Eq. (3) are in excellent agreement with experiment. (c) Polarization of W530 fitted using the generalized 3D XY model of Kost-Smith *et al.* [30].

transitions. We have developed a generalized Langevin-Debye model assuming a field-dependent molecular orientation distribution that explains quantitatively the main electro-optic and polarization reversal effects observed experimentally in the de Vries Sm-A^* phase. Allowing the tilt distribution to vary with applied field in the model gives tilt, birefringence, and polarization response curves with sigmoidal shape, characteristic of systems with first-order phase transitions.

ACKNOWLEDGMENTS

The authors thank Matthew Glaser for useful discussions and for a critical reading of the manuscript. This work was supported by National Science Foundation (NSF) Materials Research Science and Engineering Centers Grant No. DMR-0820579 and by NSF Grant No. DMR-1008300. Use of the National Synchrotron Light Source was supported by the U.S. Department of Energy, Divisions of Materials and Chemical Sciences.

APPENDIX: DERIVATION OF ELECTRIC FIELD-INDUCED TILT AND BIREFRINGENCE IN THE CHIRAL DE VRIES SMECTIC-*A* PHASE

The electro-optic experiments are carried out in the geometry shown in Fig. 2. In the molecular frame **123** where the director **n** is along the **3** axis, we may write the dielectric permittivity tensor ε as

$$\varepsilon = \begin{pmatrix} \varepsilon_1 & 0 & 0 \\ 0 & \varepsilon_2 & 0 \\ 0 & 0 & \varepsilon_3 \end{pmatrix}.$$

In order to express the dielectric tensor in the laboratory frame **xyz**, we imagine that the director **n** is initially along the **z** direction. First we rotate the director clockwise through an angle θ about the **x** axis as follows:

$$\varepsilon_{R(\theta)} = R_x(-\theta)\varepsilon R_x(\theta) = \begin{pmatrix} 1 & 0 & 0 \\ 0 & \cos\theta & \sin\theta \\ 0 & -\sin\theta & \cos\theta \end{pmatrix} \begin{pmatrix} \varepsilon_1 & 0 & 0 \\ 0 & \varepsilon_2 & 0 \\ 0 & 0 & \varepsilon_3 \end{pmatrix} \begin{pmatrix} 1 & 0 & 0 \\ 0 & \cos\theta & -\sin\theta \\ 0 & \sin\theta & \cos\theta \end{pmatrix}$$

$$= \begin{pmatrix} \varepsilon_1 & 0 & 0 \\ 0 & \varepsilon_2\cos^2\theta + \varepsilon_3\sin^2\theta & (\varepsilon_3 - \varepsilon_2)\sin\theta\cos\theta \\ 0 & (\varepsilon_3 - \varepsilon_2)\sin\theta\cos\theta & \varepsilon_2\sin^2\theta + \varepsilon_3\cos^2\theta \end{pmatrix}.$$

Then we rotate the director counterclockwise through an angle ϕ about the **z** axis to obtain the dielectric tensor in the laboratory frame,

$$\varepsilon_{R(\theta,\phi)} = R_z(\phi)\varepsilon_{R(\theta)}R_z(-\phi)$$

$$= \begin{pmatrix} \cos\phi & -\sin\phi & 0 \\ \sin\phi & \cos\phi & 0 \\ 0 & 0 & 1 \end{pmatrix} \begin{pmatrix} \varepsilon_1 & 0 & 0 \\ 0 & \varepsilon_2\cos^2\theta + \varepsilon_3\sin^2\theta & (\varepsilon_3 - \varepsilon_2)\sin\theta\cos\theta \\ 0 & (\varepsilon_3 - \varepsilon_2)\sin\theta\cos\theta & \varepsilon_2\sin^2\theta + \varepsilon_3\cos^2\theta \end{pmatrix} \begin{pmatrix} \cos\phi & \sin\phi & 0 \\ -\sin\phi & \cos\phi & 0 \\ 0 & 0 & 1 \end{pmatrix}$$

$$= \begin{pmatrix} \varepsilon_{11} & \varepsilon_{12} & \varepsilon_{13} \\ \varepsilon_{21} & \varepsilon_{22} & \varepsilon_{23} \\ \varepsilon_{31} & \varepsilon_{32} & \varepsilon_{33} \end{pmatrix},$$

where

$$\varepsilon_{11} = (\varepsilon_2\cos^2\theta + \varepsilon_3\sin^2\theta)\sin^2\phi + \varepsilon_1\cos^2\phi, \quad \varepsilon_{12} = \varepsilon_{21} = (\varepsilon_1 - \varepsilon_2\cos^2\theta - \varepsilon_3\sin^2\theta)\sin\phi\cos\phi,$$
$$\varepsilon_{13} = \varepsilon_{31} = (\varepsilon_2 - \varepsilon_3)\sin\theta\cos\theta\sin\phi, \quad \varepsilon_{22} = (\varepsilon_2\cos^2\theta + \varepsilon_3\sin^2\theta)\cos^2\phi + \varepsilon_1\sin^2\phi,$$
$$\varepsilon_{23} = \varepsilon_{32} = (\varepsilon_3 - \varepsilon_2)\sin\theta\cos\theta\cos\phi, \quad \varepsilon_{33} = \varepsilon_2\sin^2\theta + \varepsilon_3\cos^2\theta.$$

To calculate the electro-optic response of a sample for light incident along the **x** direction, we first average the dielectric tensor over the distribution function $f(\theta, \phi)$ given by the generalized Langevin-Debye model described in the text and then diagonalize the average dielectric tensor in the **yz** plane. The eigenvectors give the principal optical axes of the sample. The optical tilt angle ψ is the angle between the eigenvectors and the **y** and **z** axes. The eigenvalues give the dielectric constants along the principal optical axes.

The average dielectric tensor in the **yz** plane is

$$\varepsilon_{yz} = \begin{pmatrix} \langle\varepsilon_{22}\rangle & \langle\varepsilon_{23}\rangle \\ \langle\varepsilon_{32}\rangle & \langle\varepsilon_{33}\rangle \end{pmatrix}.$$

We can diagonalize ε_{yz} by rotating the tensor by ψ in the **yz** plane and setting the off-diagonal elements to zero as follows:

$$\begin{aligned}\varepsilon'_{yz} &= \begin{pmatrix}\cos\psi & -\sin\psi\\ \sin\psi & \cos\psi\end{pmatrix}\varepsilon_{yz}\begin{pmatrix}\cos\psi & \sin\psi\\ -\sin\psi & \cos\psi\end{pmatrix}\\ &= \begin{pmatrix}\langle\varepsilon_{22}\rangle\cos^2\psi - 2\langle\varepsilon_{23}\rangle\sin\psi\cos\psi + \langle\varepsilon_{33}\rangle\sin^2\psi & (\langle\varepsilon_{22}\rangle - \langle\varepsilon_{33}\rangle)\sin\psi\cos\psi + \langle\varepsilon_{23}\rangle\cos 2\psi\\ (\langle\varepsilon_{22}\rangle - \langle\varepsilon_{33}\rangle)\sin\psi\cos\psi + \langle\varepsilon_{23}\rangle\cos 2\psi & \langle\varepsilon_{22}\rangle\sin^2\psi + 2\langle\varepsilon_{23}\rangle\sin\psi\cos\psi + \langle\varepsilon_{33}\rangle\cos^2\psi\end{pmatrix}\\ &= \begin{pmatrix}\varepsilon'_y & 0\\ 0 & \varepsilon'_z\end{pmatrix}.\end{aligned}$$

Setting the off-diagonal elements $(\langle\varepsilon_{22}\rangle - \langle\varepsilon_{33}\rangle)\sin\psi\cos\psi + \langle\varepsilon_{23}\rangle\cos 2\psi$ to zero, yields the apparent optical tilt angle ψ,

$$\tan 2\psi = \frac{2\langle\varepsilon_{23}\rangle}{\langle\varepsilon_{33}\rangle - \langle\varepsilon_{22}\rangle} = \frac{2\langle(\varepsilon_3-\varepsilon_2)\sin\theta\cos\theta\cos\phi\rangle}{\langle\varepsilon_2\sin^2\theta + \varepsilon_3\cos^2\theta\rangle - \langle((\varepsilon_2\cos^2\theta + \varepsilon_3\sin^2\theta)\cos^2\phi + \varepsilon_1\sin^2\phi)\rangle}.$$

In order to account for the field dependence of the birefringence Δn, Selinger *et al.* [24] kept the cone angle θ_A fixed at its high field value but made the local dielectric tensor biaxial. Any optical biaxiality would be expected to show up in the Sm-C^* phase as well but this is not observed in our experiments. We therefore neglect optical biaxiality in the de Vries Sm-A^* phase and assume that $\varepsilon_1 = \varepsilon_2$, allowing us to simplify the above equation:

$$\begin{aligned}\tan 2\psi &= \frac{\langle(\varepsilon_3-\varepsilon_1)\sin 2\theta\cos\phi\rangle}{\langle\varepsilon_1\sin^2\theta + \varepsilon_3\cos^2\theta - (\varepsilon_1\cos^2\theta + \varepsilon_3\sin^2\theta)\cos^2\phi - \varepsilon_1\sin^2\phi\rangle}\\ &= \frac{\langle(\varepsilon_3-\varepsilon_1)\sin 2\theta\cos\phi\rangle}{\langle(\varepsilon_3-\varepsilon_1)\cos^2\theta - (\varepsilon_3-\varepsilon_1)\sin^2\theta\cos^2\phi\rangle}\\ &= \frac{\langle\sin 2\theta\cos\phi\rangle}{\langle\cos^2\theta - \sin^2\theta\cos^2\phi\rangle}.\end{aligned} \tag{A1}$$

This result is shown as Eq. (1) in the text.

The dielectric anisotropy for light incident along **x** is given by the difference between the diagonal elements of $\varepsilon_{yz}{}'$,

$$\begin{aligned}\Delta\varepsilon &= \varepsilon'_z - \varepsilon'_y = \langle\varepsilon_{22}\rangle\sin^2\psi + 4\langle\varepsilon_{23}\rangle\sin\psi\cos\psi + \langle\varepsilon_{33}\rangle\cos^2\psi - \langle\varepsilon_{22}\rangle\cos^2\psi - \langle\varepsilon_{33}\rangle\sin^2\psi\\ &= (\langle\varepsilon_{33}\rangle - \langle\varepsilon_{22}\rangle)\cos 2\psi + 2\langle\varepsilon_{23}\rangle\sin 2\psi = (\langle\varepsilon_{33}\rangle - \langle\varepsilon_{22}\rangle)\cos 2\psi + (\langle\varepsilon_{33}\rangle - \langle\varepsilon_{22}\rangle)\tan 2\psi\sin 2\psi\\ &= \frac{\langle\varepsilon_{33}\rangle - \langle\varepsilon_{22}\rangle}{\cos 2\psi} = \frac{\langle\varepsilon_1\sin^2\theta + \varepsilon_3\cos^2\theta\rangle - \langle((\varepsilon_1\cos^2\theta + \varepsilon_3\sin^2\theta)\cos^2\phi + \varepsilon_1\sin^2\phi)\rangle}{\cos 2\psi}\\ &= \frac{\langle\varepsilon_1 - \varepsilon_1\cos^2\theta + \varepsilon_3\cos^2\theta - \varepsilon_1\cos^2\phi + \varepsilon_1\sin^2\theta\cos^2\phi - \varepsilon_3\sin^2\theta\cos^2\phi - \varepsilon_1\sin^2\phi\rangle}{\cos 2\psi}\\ &= \frac{(\varepsilon_3-\varepsilon_1)\langle(\cos^2\theta - \sin^2\theta\cos^2\phi)\rangle}{\cos 2\psi}.\end{aligned}$$

When the applied field is very strong, the azimuthal distribution is very narrow. In this case, $\langle\cos^2\phi\rangle \approx 1$, and we obtain maximal dielectric anisotropy $\Delta\varepsilon_{max} = \varepsilon_3 - \varepsilon_1$. The scaled anisotropy then may be written

$$\frac{\Delta\varepsilon}{\Delta\varepsilon_{max}} = \frac{\langle\cos^2\theta - \sin^2\theta\cos^2\phi\rangle}{\cos 2\psi}.$$

Because $\varepsilon = n^2$ and $\Delta\varepsilon = 2\bar{n}\Delta n$, where $\bar{n} = (n_3 + n_1)/2$, we obtain

$$\frac{\Delta n}{\Delta n_{max}} = \frac{\Delta\varepsilon}{\Delta\varepsilon_{max}} = \frac{\langle\cos^2\theta - \sin^2\theta\cos^2\phi\rangle}{\cos 2\psi}. \tag{A2}$$

This expression, relating the cell birefringence to the optical tilt, appears as Eq. (2) in the text.

[1] R. B. Meyer, L. Liebert, L. Strzelecki, and P. Keller, J. Phys. Lett. **36**, 69 (1975).

[2] H. Takezoe and Y. Takanishi, Jpn. J. Appl. Phys. **45**, L597 (2006).

[3] R. A. Reddy and C. Tschierske, J. Mater. Chem. **16**, 907 (2006).

[4] R. A. Reddy, C. Zhu, R. Shao, E. Korblova, T. Gong, Y. Shen, E. Garcia, M. A. Glaser, J. E. Maclennan, D. M. Walba, and N. A. Clark, Science **332**, 72 (2011).

[5] S. T. Lagerwall, *"Ferroelectric and Antiferroelectric Liquid Crystals"*, Wiley-VCH, Weinheim (1999).

[6] A. D. L. Chandani, T. Hagiwara, Y. Suzuki, Y. Ouchi, H. Takezoe, and A. Fukuda, Jpn. J. Appl. Phys. **27**, L729 (1988).

[7] K. Miyasato, S. Abe, H. Takezoe, A. Fukuda, and E. Kuze, Jpn. J. Appl. Phys. **22**, L661 (1983).

[8] Y. Shen, T. Gong, R. Shao, E. Korblova, J. E. Maclennan, D. M. Walba, and N. A. Clark, Phys. Rev. E **84**, 020701(R) (2011).
[9] S. Garoff and R. B. Meyer, Phys. Rev. Lett. **38** 848 (1977); Phys. Rev. A **19**, 338 (1979).
[10] A. de Vries, J. Chem. Phys. **71**, 25 (1979).
[11] J. P. F. Lagerwall and F. Giesselmann, Chem. Phys. Chem **7**, 20 (2006).
[12] M. D. Radcliffe, M. L. Brostrom, K. A. Epstein, A. G. Rappaport, B. N. Thomas, R. Shao, and N. A. Clark, Liq. Cryst. **26**, 789 (1999).
[13] J. C. Roberts, N. Kapernaum, F. Giesselmann, and R. P. Lemieux, J. Am. Chem. Soc. **130**, 13842 (2008).
[14] L. Wang, D. M. Walba, R. Shao, D. A. Coleman, M. Nakata, T. Shimmachi, J. E. Maclennan, and N. A. Clark, in *Proceedings of the 21st International Liquid Crystal Conference* (Taylor & Francis, Col.) (2006).
[15] S. K. Prasad, D. S. Shankar Rao, S. Sridevi, C. V. Lobo, B. R. Ratna, J. Naciri, and R. Shashidhar, Phys. Rev. Lett. **102**, 147802 (2009).
[16] S. Ghosh, P. Nayek, S. K. Roy, T. P. Majumder, M. Zurowska, and R. Dabrowski, Europhys. Lett. **89**, 16001 (2010).
[17] A. D. L. Chandani, E. Gorecka, Y. Ouchi, H. Takezoe, and A. Fukuda, Jpn. J. Appl. Phys. **28**, L1265 (1989).
[18] K. Itoh, Y. Takanishi, J. Yokoyama, K. Ishikawa, H. Takezoe, and A. Fukuda, Jpn. J. Appl. Phys. **36** L784 (1997).
[19] M. Zennyoji, J. Yokoyama, Y. Takanishi, K. Ishikawa, H. Takezoe, and A. Fukuda, Jpn. J. Appl. Phys. **37**, 6071 (1998).
[20] J. P. F. Lagerwall, Phys. Rev. E **71**, 051703 (2005).
[21] Ch. Bahr and G. Heppke, Phys. Rev. A **39**, 5459 (1989).
[22] Ch. Bahr and G. Heppke, Phys. Rev. A **41**, 4335 (1990).
[23] N. A. Clark, D. Coleman, and J. E. Maclennan, Liq. Cryst. **27**, 985 (2000).
[24] J. V. Selinger, P. J. Collings, and R. Shashidhar, Phys. Rev. E **64**, 061705 (2001).
[25] N. A. Clark, T. Bellini, R. Shao, D. Coleman, S. Bardon, D. R. Link, J. E. Maclennan, X. Chen, M. D. Wand, D. M. Walba, P. Rudquist, and S. T. Lagerwall, Appl. Phys. Lett. **80**, 4097 (2002).
[26] P. J. Collings, B. R. Ratna, and R. Shashidhar, Phys. Rev. E **67**, 021705 (2003).
[27] A. Fukuda, *Proceedings of the 15th International Display Research Conference of the SID* (Society for Information Display, San Jose, California, 1995), p. 61; S. Inui, N. Iimura, T. Suzuki, H. Iwane, K. Miyachi, Y. Takanishi, and A. Fukuda, J. Mater. Chem. **6**, 671 (1996).
[28] P. Rudquist, J. P. F. Lagerwall, M. Buivydas, F. Gouda, S. T. Lagerwall, N. A. Clark, J. E. Maclennan, R. Shao, D. A. Coleman, S. Bardon, T. Bellini, D. R. Link, G. Natale, M. A. Glaser, D. M. Wand, and X.-H. Chen, J. Mater. Chem. **9**, 1257 (1999).
[29] K. Saunders, Phys. Rev. E **80**, 011703 (2009).
[30] Z. V. Kost-Smith, P. D. Beale, N. A. Clark, and M. A. Glaser, Phys. Rev. E **87**, 050502(R) (2013).